Science Advances

AAAS

advances.sciencemag.org/cgi/content/full/4/5/eaap8306/DC1

Supplementary Materials for

Chronology of martian breccia NWA 7034 and the formation of the martian crustal dichotomy

William S. Cassata, Benjamin E. Cohen, Darren F. Mark, Reto Trappitsch, Carolyn A. Crow, Joshua Wimpenny, Martin R. Lee, Caroline L. Smith

Published 23 May 2018, *Sci. Adv.* **4**, eaap8306 (2018)
DOI: 10.1126/sciadv.aap8306

The PDF file includes:

Other Supplementary Material for this manuscript includes the following:
(available at advances.sciencemag.org/cgi/content/full/4/5/eaap8306/DC1)

- data file S1. Complete analytical data set (Excel file).

Supplementary Materials and Methods

Sample Description

Northwest Africa (NWA) 7034 and its pairings (NWA 7475, NWA 7533, NWA 7906, NWA 7907, NWA 8114, NWA 8171, NWA 8674, NWA 10922 NWA 11220, NWA 11522, and Rabt Sbayta 003) were deposited as a strewn field in the Western Sahara. The rock is a polymict regolith breccia comprising predominantly igneous clasts set in a fine-grained (sub-micron-sized) matrix of feldspar, pyroxene, and minor accessory phases (fig. S1) (*1*). In addition to igneous lithologies, NWA 7034 contains impact melt, proto-breccia, and sedimentary clasts, and angular mineral fragments of K-feldspar, plagioclase feldspar, and pyroxene (*1, 4*). Mineral fragments are often > 1 mm in width, and clasts exceed 1 cm in width (fig. S1) (*1*). Brittle deformation, mechanical twinning, and undulatory extinction in pyroxene and plagioclase crystals indicate that the meteorite is only weakly shocked (5 – 15 GPa) (*4*). Low pressures are also indicated by the lack of conversion of plagioclase into maskelynite (*20*). The rock contains elevated concentrations of highly siderophile elements consistent with up to 5 wt.-% CI-chondrite impactor material (*25*). Fine-grained phyllosilicates, hydrous iron oxides, pyrite, and alteration of apatite and zircon indicate that the source lithologies were subjected to low temperature aqueous alteration (>100 °C to <500 °C) (*3, 4, 62, 63*). All measurements at Lawrence Livermore National Laboratory (LLNL) were conducted on material from the original NWA 7034 main mass, which was provided by Carl Agee (University of New Mexico). All measurements at the Scottish Universities Environmental Research Centre (SUERC) were conducted on material from the paired stone NWA 11522, which is a 3.2 g stone that was purchased from Darryl Pitt in November 2013; the main mass is held at the Natural History Museum, London.

$^{40}Ar/^{39}Ar$ Measurements

Whole-rock fragments and mineral separates were analyzed for $^{40}Ar/^{39}Ar$ chronometry in both the Livermore Noble Gas Lab at LLNL and the NERC Argon Isotope Facility at SUERC.

At LNNL, an approximately 125 mg fragment of NWA 7034 was gently crushed in an agate mortar and pestle and feldspars and mg-sized, visibly monomict whole-rock fragments were hand-picked for analysis. The samples were loaded into aluminum discs alongside Fish Canyon sanidine and Hb3gr hornblende neutron fluence monitors. The samples and fluence monitors were co-irradiated for 50 hours at the Oregon State University TRIGA reactor in the Cadmium-Lined In-Core Irradiation Tube (CLICIT). After a decay period of approximately three months, whole-rock fragments and mineral separates were then loaded into small metal packets made from high-purity, 6 mm long Pt-Ir (90:10) tubes (2.9 mm in diameter with a 0.15 mm wall thickness), crimped at both ends to create an encapsulating "envelope", and placed into an ultra-high vacuum system beneath a sapphire view port. Samples were heated with a 75 W diode laser (λ = 810 ± 10 nm) focused onto the metal envelope and coaxially aligned with an optical pyrometer. To account for the temperature dependent emissivity of the Pt-Ir metal, the single-color pyrometer was calibrated against a type-K thermocouple under ultra-high vacuum ($<10^{-9}$ torr) and under the same conditions as the diffusion experiments (i.e., same alloy, viewport, cover slide, and focal point). During experimental heating, the samples were held at temperatures between ~500 and 1600 °C for durations of 180 seconds. Typical durations required to reach the set-point temperatures were <10 seconds. Following heating, samples cooled to hundreds of degrees below set-point temperatures in equivalent durations. Precision on all temperature

measurements is better than 5 °C. Accuracy on type-K thermocouples is approximately 0.4% (*64*). The precision of the pyrometer-to-thermocouple calibration is ~10 °C (*65*). The released argon was purified using four SAES GP-50 getters with St101 cartridges, three at room temperature (0 A) and the other at ~150 °C (1 A), and analyzed using a Nu Instruments *Noblesse* mass spectrometer equipped with six Faraday cup detectors and four ion-counting, discrete dynode multiplier detectors. Samples were analyzed statically in peak-hopping mode using the axial multiplier detector.

At SUERC, a 248.56 mg fragment of the paired stone NWA 11522 was gently crushed in an agate mortar and pestle, and the liberated fragments of groundmass and feldspar were then washed in a mixture of distilled water and ethanol in an ultrasonic bath for approximately one hour to remove dust. Feldspars and visibly monomict whole-rock fragments that varied from light to darker grey in color were separated by hand-picking (fig. S1). These separates were then loaded into a 21-pit aluminum irradiation disk alongside Hb3gr hornblende and GA1550 biotite neutron fluence monitors. The samples and fluence monitors were co-irradiated for 40 hours at the Oregon State University TRIGA reactor in the CLICIT. After a decay period of approximately three months, analyses of neutron flux monitors and meteorite samples were undertaken on a MAP 215-50 spectrometer operated in peak-hopping mode, with measured sensitivity of ~6.5 $x10^{-15}$ moles/Volt. Single crystals/single rock fragments of NWA 11522 and age standards were placed in 2 mm diameter and 2 mm deep circular holes in a steel palette, which was loaded into a laser chamber of a noble gas ultra-high vacuum extraction line and baked at <150 °C for ~2 days. Hb3gr crystals were analyzed via total-fusion, while aliquots of NWA 11522 and GA 1550 were incrementally heated using a CO_2 laser. Samples were heated for 40 seconds per step, using a circular flat beam 2 mm in diameter. The released gases were purified in two stages, using two SAES GP-50 getters with St101 cartridges, one at room temperature (0 A) and the other at ~450 °C (2 A). Isotope extraction, purification, extraction line operation, and mass spectrometry were fully automated.

For both LLNL and SUERC $^{40}Ar/^{39}Ar$ data, corrections were made for interfering nuclear reaction products (*66*), cosmogenic ^{36}Ar and ^{38}Ar (*67*), ^{37}Ar and ^{39}Ar decay, spectrometer discrimination, and extraction line blanks. Mass discrimination was monitored via analyses of atmospheric Ar aliquots from an automated pipette system, interspersed with the unknowns. Mass discrimination was calculated per AMU using the power law, the average $^{40}Ar/^{36}Ar$ value from the pipette analyses, and an atmospheric $^{40}Ar/^{36}Ar$ value of 298.56 ± 0.31 (*68*). Ages were calculated using the decay constants and standard calibration of (*69*).

He, Ne, Ar, Kr, and Xe Measurements

Helium, Ne, Ar, Kr, and Xe isotopes were analyzed in un-irradiated, polymict whole-rock fragments in the Livermore Noble Gas Lab to calculate U-Th-Sm/He, U-Pu/Xe, and cosmic ray exposure ages, and to determine the isotopic composition of trapped noble gas components. Argon, Kr, and Xe data from LLNL-UI-1, -2, and -3 are from (*16*). Whole-rock fragments were loaded into Pt-Ir metal packets, incrementally heated with a 75 W diode laser, and measured statically in peak hopping mode using the axial multiplier detector, as described above. Sample analyses were bracketed by measurements of a spike of known abundance and isotopic composition to monitor for time dependent changes in spectrometer sensitivity and mass

discrimination. Detailed descriptions of Ar, Kr, and Xe data reduction procedures are given in (*16*).

Exposure ages were calculated from the element production rates given in (*24*) using the chemical composition determined by inductively coupled plasma mass spectrometry (see the Supplementary Files). All ^{21}Ne was assumed to be cosmogenic.

U-Th-Sm/He ages were calculated from the sample-specific U, Th, and Sm concentration measurements. Data were corrected for cosmogenic ^{4}He assuming a cosmogenic ^{4}He/^{3}He ratio of 5.2 ± 0.3 (*70*).

U-Pu/Xe ages were calculated from the sample-specific U and Nd concentration measurements. Fissiogenic Xe abundances were determined on a step-wise basis using the following approach. A two-component deconvolution of the cosmogenic corrected ^{132}Xe/^{129}Xe ratio was performed to calculate the solar and atmospheric abundances of ^{129}Xe in each step, assuming solar ^{129}Xe/^{132}Xe = 1.0405 ± 0.0010 (*71*) and atmospheric ^{129}Xe/^{132}Xe = 2.140 ± 0.032 (*16*). Minor (<5%) contributions of fissiogenic ^{132}Xe were neglected in this calculation. Proportional abundances of solar and atmospheric ^{136}Xe were then subtracted from the total measured ^{136}Xe in each extraction. The remaining ^{136}Xe was assumed to be derived from spontaneous fission of ^{238}U and ^{244}Pu. The following constants were used in age and uncertainty calculations: ^{244}Pu half-life = 81.8 ± 0.37 Ma (*72*), ^{244}Pu spontaneous fission branching fraction = 0.00125 ± 0.00006 (*72*), ^{136}Xe cumulative yield from spontaneous fission of ^{244}Pu = 5.6 ± 0.5% (*73*), ^{238}U half-life = 4468 ± 2 Ma (*74*), ^{238}U spontaneous fission branching fraction = 5.45 ± 0.12 x 10^{-7} (*75*), and ^{136}Xe cumulative yield from spontaneous fission of ^{238}U = 6.7 ± 0.5% [(*76*), based on branching ratio of (*75*)]. Neutron-induced fission of ^{235}U was neglected given the low thermal neutron fluence inferred from the abundances of ^{80}Kr and ^{82}Kr produced by neutron capture on ^{79}Br and ^{81}Br, respectively (discussed in more detail below).

Major, Minor, and Trace Element Concentration Measurements

Elemental concentration analyses were performed at LLNL using a Thermo Scientific Element XR inductively coupled plasma mass spectrometer (ICP-MS) following techniques previously described in (*77*). After noble gas extractions, samples LLNL-UI-1, -2, -3, -4, and -5 were digested using ultra-pure concentrated acids (HF-HNO_3-HCl) for U (discussed below), Th, Sm, and Nd concentration measurements. Additionally, an aliquot was dissolved for major, minor, and trace element concentrations, the results of which were used to calculate exposure ages. Aliquots of the solutions were weighed, dried down in Teflon beakers, and diluted in 2% HNO_3 that was spiked with an internal standard consisting of a 1 ppb mixture of ^{115}In, ^{187}Re, and ^{209}Bi. Signal intensities of the internal standard isotopes were used to correct for instrumental sensitivity changes throughout the analyses. Concentrations were calculated by normalizing background and drift corrected intensities to a calibration curve prepared on the day of the analytical run. This calibration curve was created using a set of serial dilutions of concentration standards provided by Inorganic Ventures. To determine measurement accuracy and reproducibility, the USGS rock standard BCR-2 and water standard NIST 1640a were analyzed along with the samples. Based on the accuracy of these standards, typical uncertainties for trace element analyses are better than 10%.

Uranium concentrations were measured by isotope dilution using a high purity ^{233}U spike previously used at LLNL (*77-79*). In order to reduce mass bias effects related to sample matrix and to remove potential isobaric and molecular interferences, the spiked samples were processed through ion exchange chromatography following methods described in (*79*). In brief, samples were dissolved in 4 M HNO_3 and loaded onto Bio-Rad poly-prep columns containing 1.8 mL of Eichrom U-TEVA resin. Matrix elements were washed through with successive elutions of 4 M HNO_3, 9 M HCl and 5 M HCl while U remained sorbed to the resin. Following elution of sample matrix, uranium was eluted from the resin using 0.1 M HCl, and the eluate was dried down. Samples were then dissolved in 9 M HCl and loaded onto a Bio-Rad poly-prep column containing 1.8 mL of BioRad AG-1 X8 anion resin. Matrix elements were eluted using 9 M HCl, and U was eluted in 0.1 M HCl. The eluate containing U was dried down and dissolved twice in ~20 μL of concentrated HNO_3 before being dissolved in 3 mL 3% HNO_3. At this point, samples were ready for analysis by ICP-MS. Uranium isotopic analyses were performed using the Element XR single collector ICP-MS at LLNL. The analytical routine involved measurement of ^{233}U, ^{234}U, ^{235}U, ^{236}U and ^{238}U in ion counting mode, with typical ^{238}U intensities in samples and standards of 2×10^6 cps. Each analysis consisted of 100 measurements with 5 s integration times. Samples were blank-corrected and then mass bias correcting using the NBL U100 uranium isotopic standard. To assess the accuracy of the measurements, the USGS standards RGM-2 and BHVO-2 were measured as unknowns, obtaining uranium concentrations of 5.46 ± 0.04 and 0.40 ± 0.01 respectively, which are within uncertainty of published values (e.g., *80*).

Statistical Analysis Methods

All uncertainties on U-Th-Sm/He, $^{40}Ar/^{39}Ar$, U-Pu/Xe, and exposure ages are reported at 2σ. Likewise, uncertainties on the trapped $^{40}Ar/^{36}Ar$ ratios inferred from isochron regressions are reported at 2σ. Uncertainties on weighted averages are reported at the 95% confidence interval (2σ analytical uncertainties expanded, if necessary (when the probability of fit <0.10), by the Student's t x $MSWD^{1/2}$.

Our criteria for an acceptable $^{40}Ar/^{39}Ar$ isochron were as follows. An isochron (1) includes the maximum number of consecutive steps with a probability of fit >0.10, (2) consists of 3 or more consecutive steps that contain > 50% of the ^{39}Ar released from the feldspathic portion of the age spectrum, and (3) has a trapped $^{40}Ar/^{36}Ar$ ratio >0. Initial low-temperature extractions that are generally imprecise and prone to terrestrial atmospheric contamination were excluded from isochron regressions (see the complete analytical data tables for omitted steps). Feldspathic portions of the age spectra were defined as those extractions that precede the generally abrupt increase in Ca/K observed on all whole-rock age spectra, or all extractions in the case of feldspar analyses. All isochron regressions were calculated using *Isoplot* (*81*) and plotted using a modified version of the MATLAB® code written by (*82*).

Our criteria for an acceptable $^{40}Ar/^{39}Ar$ plateau were as follows. A plateau (1) includes the maximum number of consecutive steps with a probability of fit >0.10, (2) consists of 3 or more consecutive steps that contain >50% of the ^{39}Ar released from the feldspathic portion of the age spectrum, (3) has no resolvable slope, and (4) has no outliers or age trends at its initial and final steps (*81*). All plateau ages were calculated using *Isoplot* (*81*).

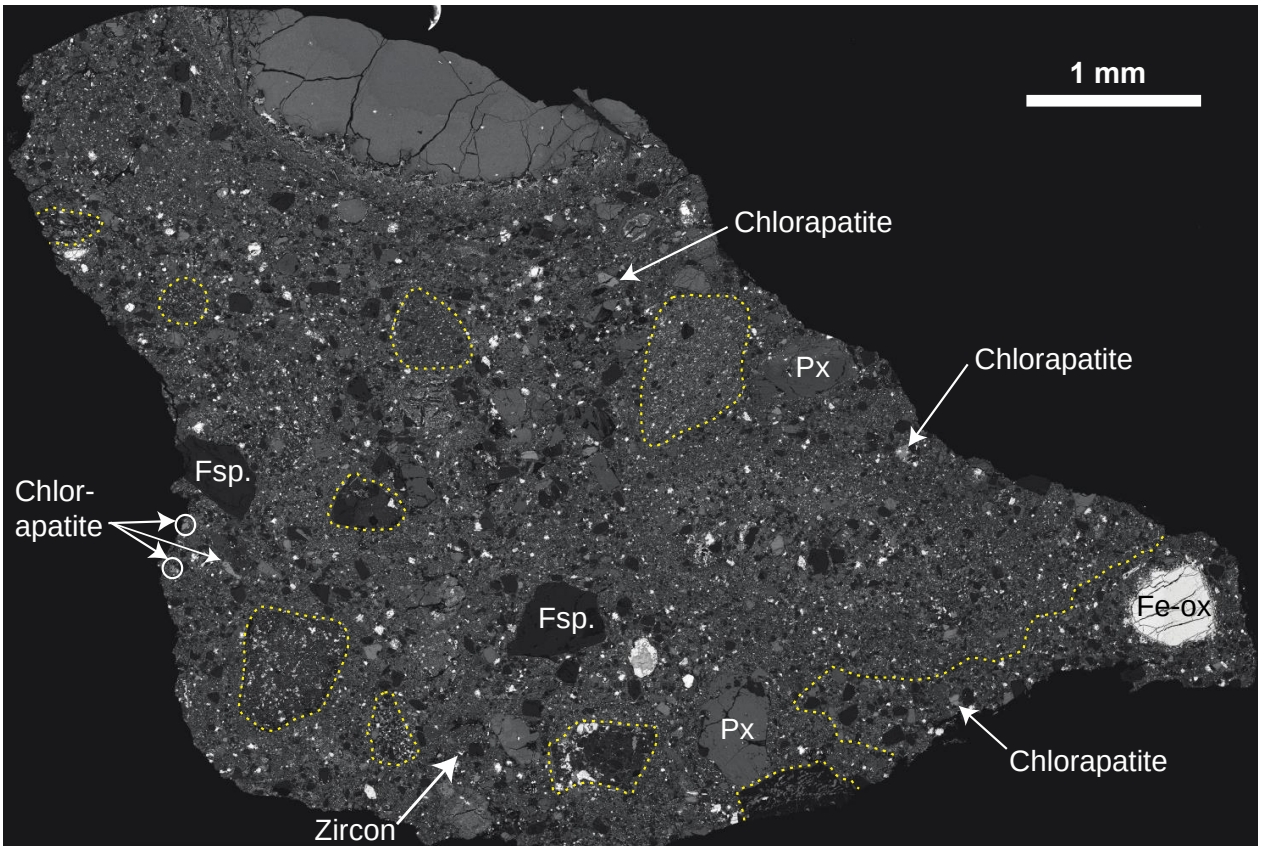

fig. S1. Image of NWA 11522. Scanning electron microscope backscattered electron micrograph showing representative monomict fragments that were targeted for $^{40}Ar/^{39}Ar$ measurements outlined in yellow.

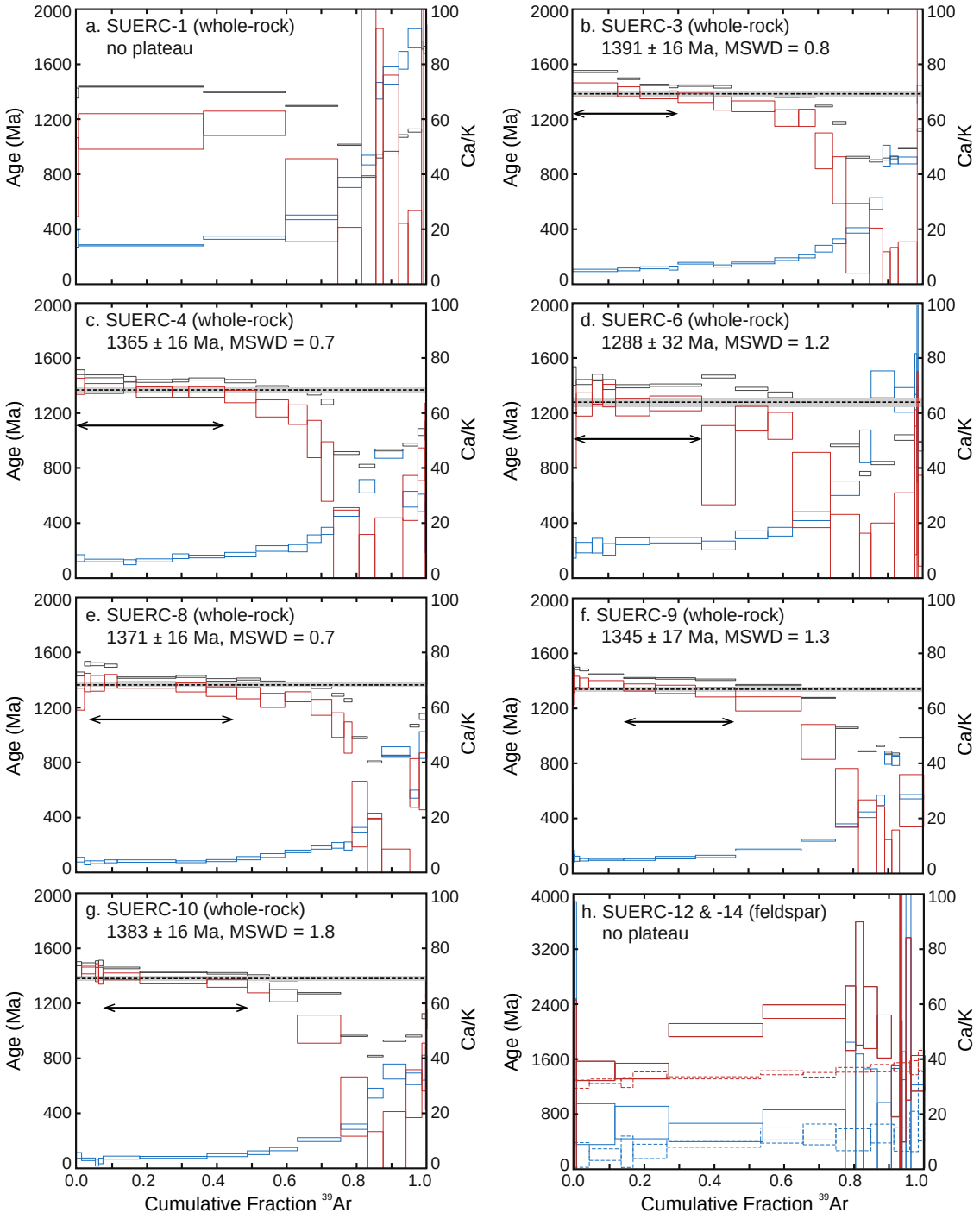

fig. S2. $^{40}Ar/^{39}Ar$ age spectra. Age and Ca/K spectra obtained from whole-rock fragments and feldspar separates. $^{40}Ar/^{39}Ar$ ages are shown without and with Martian atmospheric corrections as gray and red boxes, respectively, and are plotted against the primary y-axis. Ca/K spectra are shown in blue and are plotted against the secondary y-axis. Each spectrum is plotted against the cumulative release fraction of ^{39}Ar. Vertical dimensions of the boxes reflect the ±2σ analytical uncertainties. The horizontal dashed black lines and associated gray bands reflect the plateau ages and their associated 2 S.E. uncertainties, respectively. Horizontal arrows denote steps that were included in plateau ages. In Panel H, SUERC-12 and -14 data are shown as solid and dashed symbols, respectively.

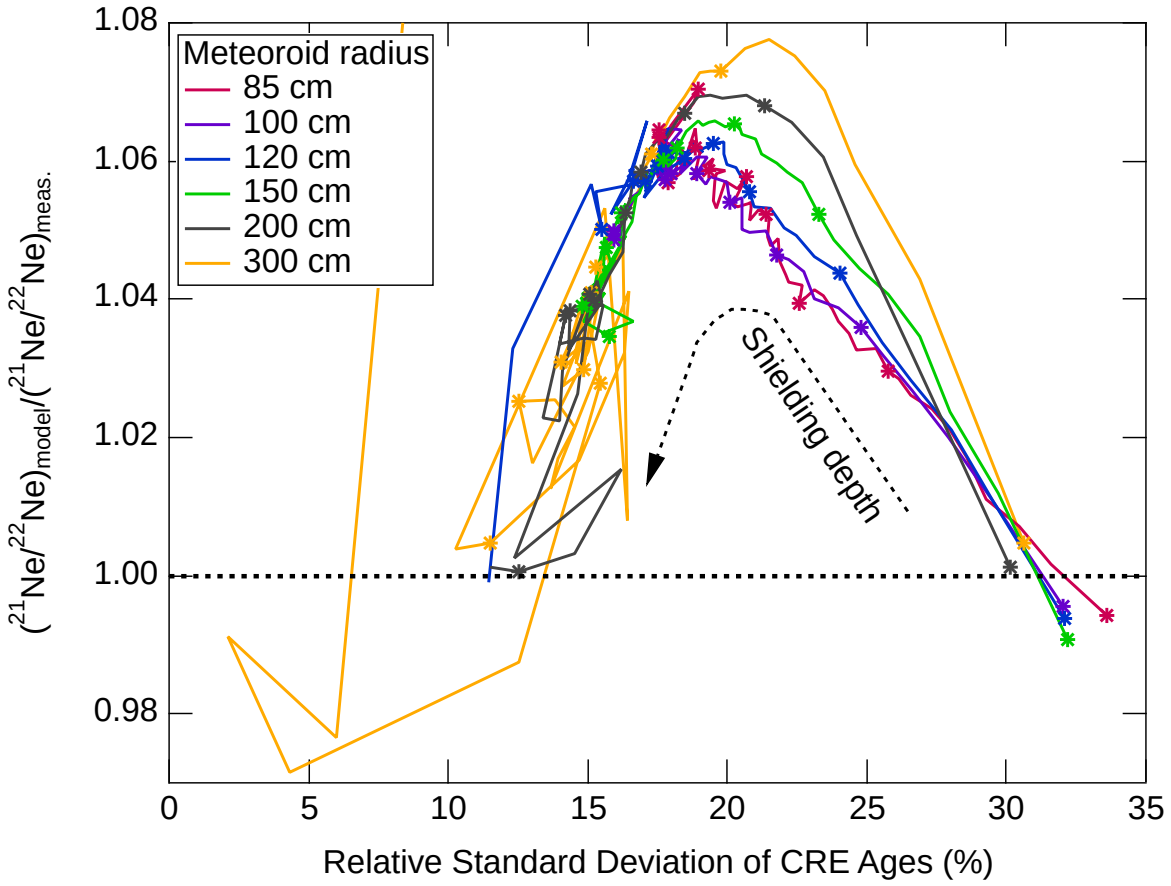

fig. S3. Irradiation modeling of NWA 7034. Plot of the modeled cosmogenic $^{21}Ne/^{22}Ne$ ratio vs. the relative standard deviation of the ^{3}He, ^{21}Ne, and ^{38}Ar exposure ages, calculated based on the depth-dependent production rates using the measured cosmogenic nuclide abundances, for a range of meteoroid sizes at various shielding depths (colored lines). The modeled $^{21}Ne/^{22}Ne$ ratio is shown relative to the measured $^{21}Ne/^{22}Ne$ ratio (i.e., a value of 1 indicates the model is indistinguishable from the measurement). The ±1σ uncertainty envelope on the measured $^{21}Ne/^{22}Ne$ ratio is represented by the vertical dimensions of the gray box. Depth of shielding within a given meteoroid increases from the start of the line on the right side of the figure to the end of the line toward the left side of the figure, as denoted by the dashed black line and arrow. The asterisk symbols (*) denote depth within the meteoroid at intervals of 10% from 0% to 100%. Production rate estimates are from (*37*). In general, the measured $^{21}Ne/^{22}Ne$ ratio and relative standard deviation between the ^{3}He, ^{21}Ne, and ^{38}Ar exposure ages are minimized when irradiation occurs toward the center of large (>100 cm) meteoroids (see text for additional discussion).